Eurasian Chem.-Technol. J. 28 (2026) 105–116
The journal of the Institute of Combustion Problems https://ect-journal.kz

https://doi.org/10.18321/ectj1687

Investigation of the Electrochemical Performance of Supercapacitor Pouch Cells in Hybrid and Symmetric Configurations using Aqueous Electrolytes

Kamila Temirkulova[1,2], Aigul Tugelbayeva[2], Balaussa Balgabayeva[1,2], Bekzat Khamzin[1,2], Sami Ullah Khan[3], Zhazira Supiyeva[1,2]*

[1]Al-Farabi Kazakh National University, 71 Al-Farabi Ave., 050040, Almaty, Kazakhstan
[2]Satbayev University, 22a Satpaev Str., 050013, Almaty, Kazakhstan
[3]Paracelsus Medical University, Strubergasse 21, 5020 Salzburg, Austria

Article info

Received:
21 November 2025

Received in revised form:
5 February 2026

Accepted:
30 April 2026

Keywords:
Supercapacitor
Aqueous electrolyte
Redox processes
Hybrid capacitance
Pouch cell

Abstract

This paper reports the electrochemical characteristics of supercapacitor pouch cells assembled on the basis of activated carbon YP80F and two types of aqueous electrolytes: 5 M LiTFSI + 0.5 M NaI (redox-active electrolyte) and 10 M LiTFSI (neat electrolyte). A comparative analysis was performed using cyclic voltammetry (CV) and galvanostatic charge-discharge (GCPL) methods in the voltage range from 0.6 to 1.5 V. It was found that the system with the addition of NaI demonstrates pronounced effects on overall performance due to reversible I^-/I_2 redox processes, which provides an increase in specific capacitance to 128 F/g and energy to 9.26 W·h/kg at a voltage of 1.5 V while maintaining high Coulombic efficiency (>97%). In contrast, the supercapacitor with 10 M LiTFSI electrolyte exhibits classic electric double layer (EDL) behavior and lower specific capacitance (64 F/g) but high stability and reversibility (efficiency >99%). A comparative analysis showed that the hybrid supercapacitor pouch cell with NaI is more promising for tasks requiring high energy density, while concentrated LiTFSI-based system is preferable for applications focused on durability and stability. The results obtained contribute to the understanding of charge accumulation mechanisms in aqueous supercapacitors and open up prospects for optimizing their characteristics depending on the target operating conditions. The results highlight that the 5 M LiTFSI + 0.5 M NaI electrolyte enhances energy density through I^-/I_2 redox reactions, while the 10 M LiTFSI system offers superior stability, demonstrating a trade-off between energy density and long-term performance.

1. Introduction

In recent decades, growth in global energy consumption, depletion of fossil fuels, and stricter environmental requirements have stimulated the active development of energy storage technologies. Traditional sources such as coal, although highly energy-dense and readily available, pose serious environmental risks when burned. In 2019 alone, coal consumption in China amounted to about 2.81 billion tons, which exceeds 40% of the global level, and coal's contribution to electricity generation remains dominant (more than 50%). Emissions of nitrogen and sulfur oxides, heavy metals, and CO_2 increase the environmental burden, so in the context of the move toward carbon neutrality, alternative approaches to coal use, including its processing into functional materials, are becoming particularly important [1].

Supercapacitors occupy an important place among energy storage devices, combining the advantages of batteries and classic capacitors: high power, long service life, fast charging, and environ-

*Corresponding author.
E-mail address: zhazira.supiyeva@gmail.com

mental safety [2, 3]. In renewable energy systems and smart grids, they act as a buffer, compensating for the instability of generation [4]. However, the key limitation for widespread implementation remains their low specific energy, which motivates the search for new electrode materials and electrolytes. Porous carbons (PCs) are important component of supercapacitors and they are mostly obtained from coal or biomass. Their high specific surface area, controllable pore architecture, and stable physicochemical properties make PCs a versatile material for energy storage systems [5, 6]. Additional interest in PC is related to its ability to absorb electromagnetic waves, which expands its range of applications. Thermal processing of biomass provides an environmentally and economically viable synthesis route, while optimization of the porous structure, increase in surface area, and introduction of multicomponent systems can significantly improve electromagnetic absorption efficiency and electrochemical characteristics [7].

From the perspective of materials science design, carbon materials with developed porosity are the basis for highly efficient electric double layer (EDL) systems. Porous carbon from coal is considered a competitive alternative to more expensive materials such as graphene [8], metal-organic frameworks [3], transition metals [9], and conductive polymers [10]. The complex properties of the raw material make coal a promising source for the synthesis of PC with the required pore architecture [11]. The choice of electrolyte, which determines ion transport, electrochemical stability, and the operating voltage window, is equally critical. Among organic, ionic liquid, and aqueous systems, the latter stand out for their high ionic conductivity, low cost, and environmental safety [12]. However, the limited voltage window of aqueous electrolytes hinders the growth of energy density. One effective way to compensate for this is to introduce redox-active additives: iodide-containing systems (I^-/I_2) participate in reversible electrochemical processes and provide an additional contribution to capacitance [5].

To gain a fundamental understanding of charge accumulation processes in supercapacitors, three-electrode cells are traditionally used, allowing separate control of the behavior of the working and auxiliary electrodes. However, for practical devices, it is more informative to study symmetric and hybrid two-electrode systems. Symmetric electric double-layer capacitor (EDLC) configurations provide high stability and efficiency but are limited in terms of specific energy, while hybrid systems combining carbon and redox-active components demonstrate higher energy density and promise for portable electronics and transportation [13, 14]. Such redox electrolytes switch the supercapacitor to hybrid mode, combining charge storage mechanisms based on EDL and Faradaic processes characteristic of battery systems. This expands the functionality of the device, increases energy efficiency, and brings its parameters closer to those of battery technologies [6, 15]. In this context, iodide-containing aqueous electrolytes are a key link in the transformation of classical supercapacitors into hybrid storage devices.

The relevance of this research is due to the need for new-generation energy sources that combine high specific energy with durability and operational safety. Supercapacitors already demonstrate high power, short charge-discharge times, and exceptional cycle stability, but the specific energy barrier requires materials science and electrochemical solutions at the electrolyte and interface levels [16–24]. Few studies have explored highly concentrated iodide-based aqueous electrolytes for pouch cell supercapacitors, and a systematic analysis of their physicochemical and electrochemical properties remains limited.

This work investigates the influence of the composition of the aqueous electrolyte on the electrochemical characteristics of YP80F-based supercapacitor cells. A comparison of two systems was carried out: a hybrid system based on 5 M LiTFSI + 0.5 M NaI and a traditional system based on 10 M LiTFSI. This comparison allows us to identify the advantages and limitations of each configuration from increasing specific energy through reversible I^-/I_2 processes to ensuring high stability in the classic EDLC mode and thus clarify the mechanisms of charge accumulation and directions for optimizing aqueous supercapacitors for specific operational requirements.

2. Materials and methods

2.1. Materials

Commercial activated carbon YP80F (Kuraray Co., Ltd., Tokyo, Japan) was used as the electrode material due to its large surface area (~2300 m^2/g) and developed porous structure, which ensure efficient charge storage in the electric double layer.

Two aqueous electrolytes were studied: 10 M lithium bis(trifluoromethanesulfonyl)imide (LiTFSI, Sigma-Aldrich, St. Louis, USA) and 5 M LiTFSI + 0.5 M sodium iodide (NaI, Sigma-Aldrich, St. Louis, USA). Concentrated LiTFSI solutions are known for their wide electrochemical stability window and high ion-

ic conductivity, making them suitable for EDLC-type supercapacitors. The addition of NaI introduces a reversible I^-/I_2 redox pair, increasing the capacitance.

To prevent short circuits while maintaining ion transport, a commercial porous polypropylene separator was used. Aluminum foil was used as the current collector, providing mechanical stability and electronic conductivity.

To evaluate the reproducibility of the pouch cell fabrication, multiple cells were assembled under identical conditions using the same electrode and electrolyte materials. Electrochemical testing, including cyclic voltammetry and galvanostatic charge–discharge, demonstrated consistent performance across all cells, with minimal variation in specific capacitance, energy density, and Coulombic efficiency. This confirms that the fabrication procedure is reliable and that the observed electrochemical behavior is reproducible, thereby supporting the robustness of the reported results.

2.2. Electrode preparation

The electrodes were prepared by mixing 90% by weight of activated carbon YP80F, 5% by weight of conductive carbon (C65 Timcal, Bodio, Switzerland), and 5% by weight of polytetrafluoroethylene binder (PTFE 60% aqueous dispersion, Sigma-Aldrich, St. Louis, USA). The homogeneous mixture was applied to aluminum foil, dried at 90 °C, and then pressed to improve adhesion and mechanical stability.

2.3. Assembly of pouch cells

The pouch-type cells were assembled in a dry atmosphere using a laminated aluminum foil casing. Each cell consisted of two prepared carbon electrodes, a polypropylene separator impregnated with the electrolyte, and an aluminum-laminated pouch casing. The cells were sealed by heat-sealing to prevent electrolyte leakage and minimize air exposure.

The precise electrode area, pouch dimensions, and sealing temperature/pressure were not recorded during the experimental work. However, the assembly procedure follows standard laboratory practices for pouch cells as described in the literature [15, 16]. For example, Safitri et al. described pouch cells with carbon-based electrodes and polypropylene or cellulose separators, packaged in laminated pouch casings with attention to sealing integrity and electrolyte containment [15]. Similarly, Chakrabarti et al. in their work reported typical mass loadings, electrode thickness, and pouch casing formats for scalable pouch supercapacitors [16].

2.4. Characterization methods

Raman spectra were recorded using a combined Raman–AFM system (Horiba LabRAM, Kyoto, Japan) equipped with a 532 nm excitation laser to analyze the degree of ordering and surface defects in the carbon framework. Scanning electron microscopy (SEM) was performed using a JSM-IT800 microscope (JEOL Ltd., Tokyo, Japan) operated at 5 kV to examine surface morphology and particle distribution. Transmission electron microscopy (TEM) images were acquired using a JEM-1400 Plus microscope (JEOL Ltd., Tokyo, Japan) at an accelerating voltage of 80 kV to observe nanoscale texture and edge structure of carbon particles. X-ray photoelectron spectroscopy (XPS) using a NEXSA spectometer (Thermo Scientific, Waltham, MA, USA) was performed with a monochromated low-power Al Kα X-ray source – 1486.6 eV.

3. Results and Discussion

Raman spectroscopy was used to analyze the structural changes in the carbon electrodes after assembling pouch cells with different electrolytes. Figure 1 shows the Raman spectra of carbon electrodes with 5 M LiTFSI + 0.5 M NaI and 10 M LiTFSI electrolytes. For both systems, the characteristic D and G bands are observed at approximately 1324 cm^{-1} and 1577 cm^{-1}, corresponding to the disordered and graphitic regions of the carbon structure. In the case of the 10 M LiTFSI electrolyte, the G band dominates, indicating a more ordered graphitic structure, while for 5 M LiTFSI + 0.5 M NaI, the more intense D band reflects an increased number of structural defects caused by the involvement of iodide and triiodide ions in surface processes. An additional band at around 842 cm^{-1} is associated with surface functional groups, and a weak 2D mode near 2673 cm^{-1} confirms partial graphitization of the material. Thus, the addition of NaI increases the defectiveness of the carbon framework, while the concentrated LiTFSI electrolyte helps preserve a more ordered carbon structure, which correlates with its improved electrochemical stability.

SEM images show flake-like activated carbon particles with interparticle voids (meso- and macro-scale gaps) in both electrodes (Fig. 2). The 10 M LiTFSI sample appears more compact, with smoother platelet surfaces and fewer loose fine particles. The 5 M LiTFSI + 0.5 M NaI sample shows slightly rougher flakes and more small debris and bridges between particles, indicating higher surface heterogeneity.

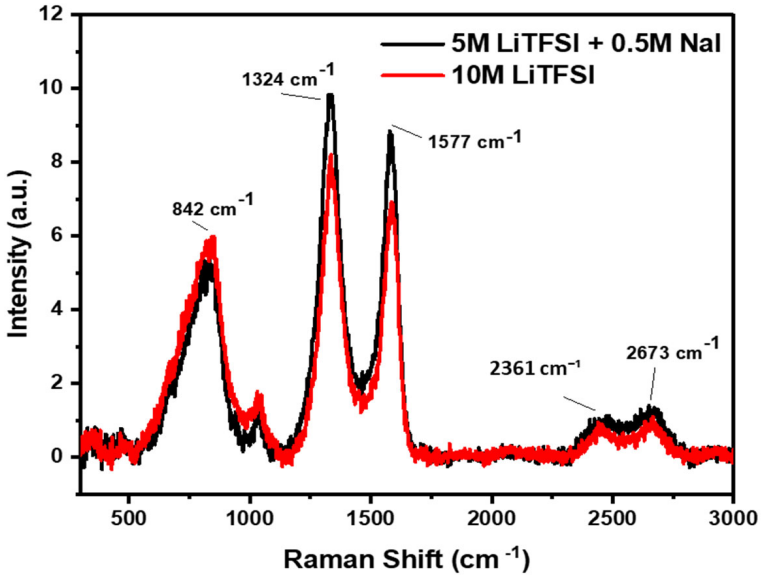

Fig. 1. Raman spectra of carbon electrodes extracted from pouch cells with 5 M LiTFSI + 0.5 M NaI and 10 M LiTFSI electrolytes.

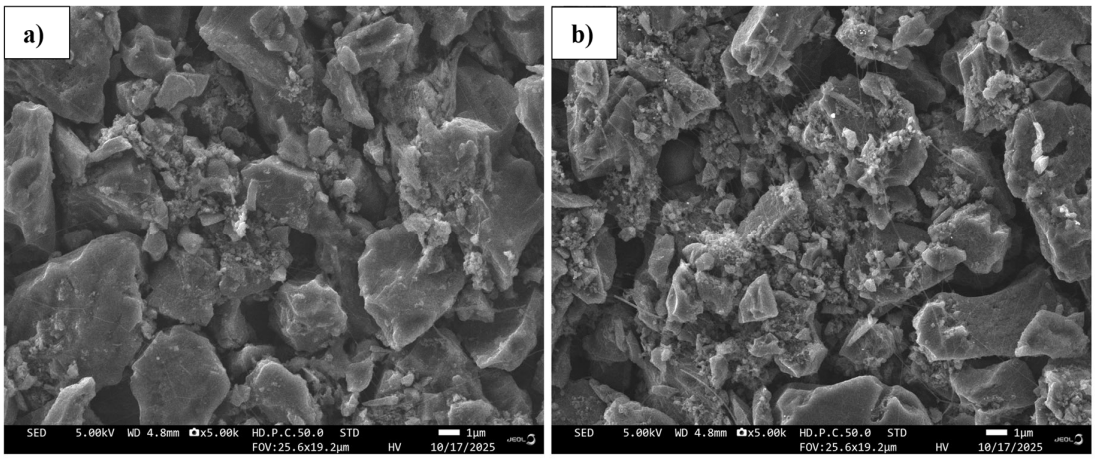

Fig. 2. SEM images of carbon electrodes: a) 5 M LiTFSI + 0.5 M NaI; b) 10 M LiTFSI.

Transmission electron microscopy (TEM) was used to study the microstructure of activated carbon electrodes (Fig. 3). The electrode from the 5 M LiTFSI + 0.5 M NaI system has thin, corrugated, and less compact carbon fragments with uneven edges, indicating a higher degree of structural disorder, possibly caused by redox changes on the surface in the presence of iodide compounds. In contrast, the electrode from the 10 M LiTFSI system has denser and more continuous carbon edges, reflecting a higher degree of structural order typical of stable EDLC-type materials.

The chemical structure information was obtained from X-ray photoelectron spectroscopy (XPS) analysis of activated carbon after immersion in the electrolyte in 10 M LiTFSI electrolyte (Fig. 4a, b). The C 1s spectrum was deconvoluted into several components corresponding to different chemical bonds. In addition to the main C–C/C=C peak located at ~284.6 eV, representing the unoxidized sp^2 domains, several peaks associated with oxygen-containing functional groups were identified: C–O (~286.2 eV), C=O (~287.7 eV), and O–C=O (~289.0 eV).

XPS analysis of activated carbon after treatment in 5 M LiTFSI + 0.5 M NaI electrolyte (Fig. 4c, d) revealed a noticeable decrease in the intensity of peaks corresponding to oxygen-containing functional groups (C–O, C=O), suggesting that part of the oxygen-containing species reacted with iodide and was removed from the surface of the material. Accordingly, the intensity of the peak associated with sp^2-hybridized carbon (C–C/C=C) increased.

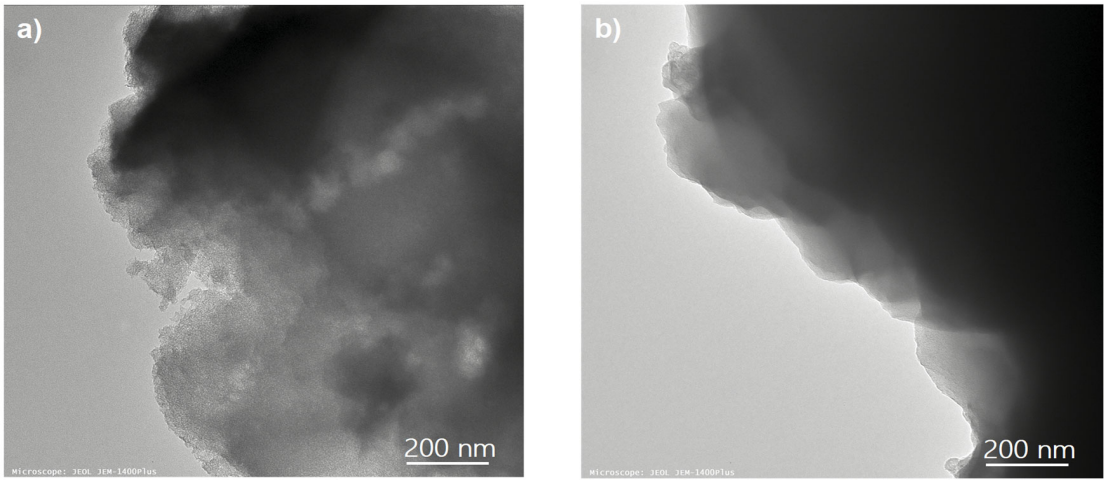

Fig. 3. TEM images of activated carbon electrodes from pouch cells with electrolytes: a) 5 M LiTFSI + 0.5 M NaI; b) 10 M LiTFSI.

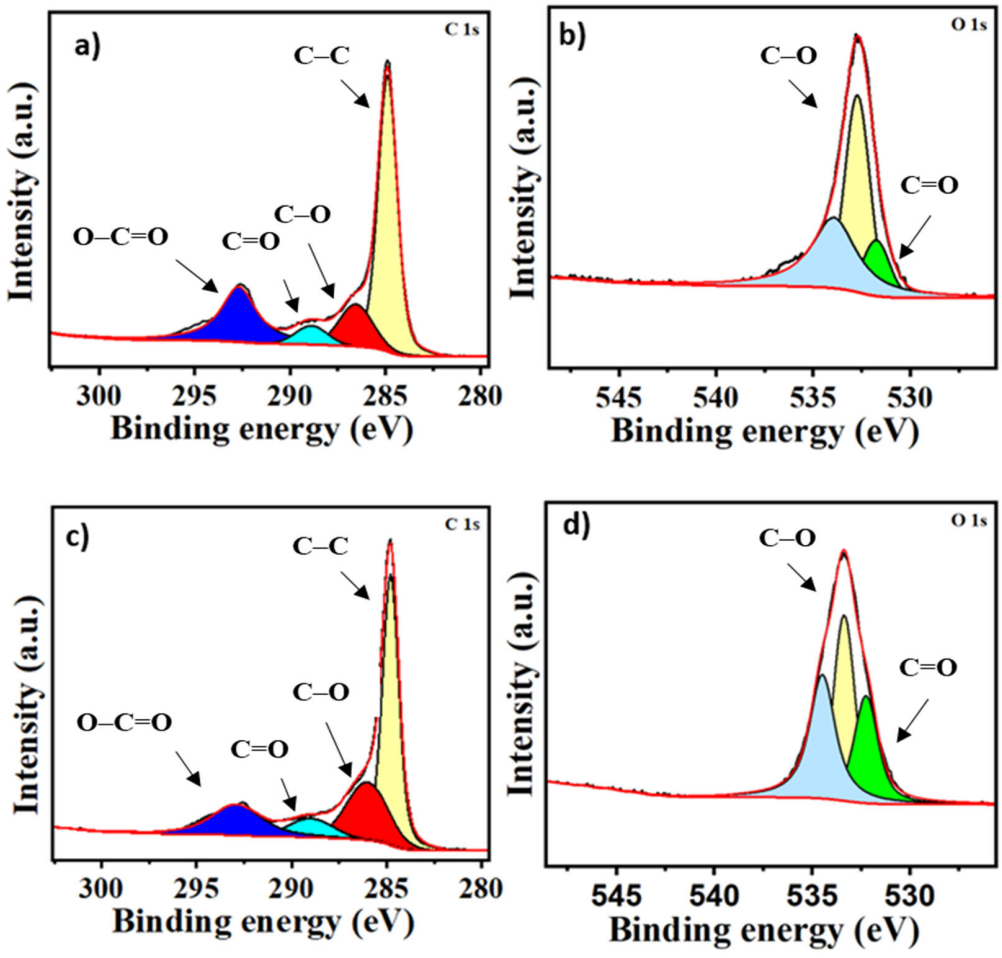

Fig. 4. XPS data of activated carbon electrodes from pouch cells with electrolytes: a), b) 10 M LiTFSI; c), d) 5 M LiTFSI + 0.5 M NaI.

The O 1s spectra (Fig. 4b, d) show peaks centered at ~531.7 eV (C=O) and ~533.2 eV (C–O), which also decrease after treatment in iodide-containing electrolyte.

Thus, the combined results obtained from all characterization methods confirm the modification of the carbon structure upon interaction with different aqueous iodide-based electrolytes.

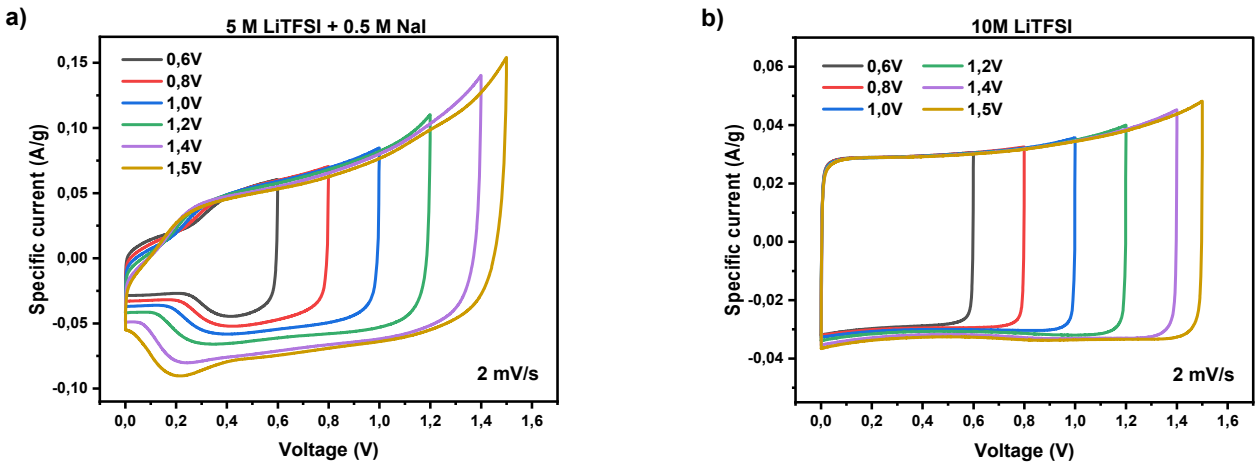

Fig. 5. Cyclic voltammetry curves of pouch cells with a) 5 M LiTFSI + 0.5 M NaI; b)10 M LiTFSI electrolytes at a scan rate of 2 mV/s in different voltage ranges (0.6–1.5 V).

Cyclic voltammetry (CV) is one of the basic methods for analyzing supercapacitors, allowing the nature of charge accumulation to be assessed and the involvement of additional processes to be identified. In this work, CV studies of stacked cells were performed at a scanning rate of 2 mV/s in various voltage ranges (0.6–1.5 V), which made it possible to sequentially track the transition from classical EDLC behavior to hybrid mechanisms. The results are shown in Fig. 5. CV curves for the 5 M LiTFSI + 0.5 M NaI electrolyte (Fig. 5a) show a characteristic expansion of the loop area with increasing upper voltage. At voltages of 0.6–0.8 V, the shape of the curves is close to an ideal rectangle, which corresponds to the electric double layer mechanism. However, starting at 1.0 V, deviations from the rectangular shape and characteristic shoulders associated with reversible I^-/I_2 redox processes appear on the curves [17–20].

With further expansion of the window to 1.4–1.5 V, the loop area increases significantly, reflecting an increase in specific capacitance. Thus, its value increases from 73 F/g at 0.6 V to 128 F/g at 1.5 V. The increase in capacitance is accompanied by the preservation of high Coulombic efficiency (~98%), which confirms the reversibility of redox processes and the stability of the system even at extended voltages. Thus, the addition of NaI transforms the system from a symmetric EDLC into a hybrid supercapacitor, where, along with electrostatic charge accumulation, a significant contribution of pseudocapacitance is realized due to I^-/I_2 transitions.

CV curves for 10 M LiTFSI electrolyte (Fig. 5b) also show an increase in loop area with increasing voltage, but the shape of the curves remains close to rectangular over the entire range. This indicates the dominance of the classical EDLC mechanism without significant involvement of redox processes. When the voltage is increased to 1.4–1.5 V, only minor distortions in shape and an increase in current are observed, which may be associated with side reactions or a minimal contribution of pseudocapacitance. Nevertheless, the specific capacitance increases only from 58 F/g at 0.6 V to 66 F/g at 1.5 V, which is significantly lower than in the NaI system. At the same time, the coulombic efficiency remains exceptionally high (>99%), reaching 100.2% at 0.6 V, which confirms the stability and reversibility of the processes in concentrated LiTFSI. Cyclic voltammetry curves (Fig. 6) of pouch cells with 5 M LiTFSI + 0.5 M NaI and 10 M LiTFSI electrolytes at a scan rate of 2 mV/s in different voltage ranges: Fig. 6a (0.6 V), where the hybrid electrolyte already demonstrates an increased loop area associated with the onset of I^-/I_2 redox activity; Fig. 6b (1.0 V), where the pseudocapacitive contribution becomes more pronounced and the CV loops expand, confirming the hybrid nature of charge accumulation; Fig. 6c (1.5 V), where redox processes dominate the response and the hybrid electrolyte shows significantly higher current values compared to the nearly rectangular EDLC-type curves of the 10 M LiTFSI system.

The 10 M LiTFSI electrolyte, on the other hand, demonstrates classic EDLC behavior: the shape of the curves remains close to rectangular over the entire voltage range, side processes are minimal, and Coulombic efficiency reaches record values (>99%). This makes it a benchmark system in terms of stability, although the capacitance and energy values remain significantly lower than those of the hybrid electrolyte. Thus, the CV results show that the addi-

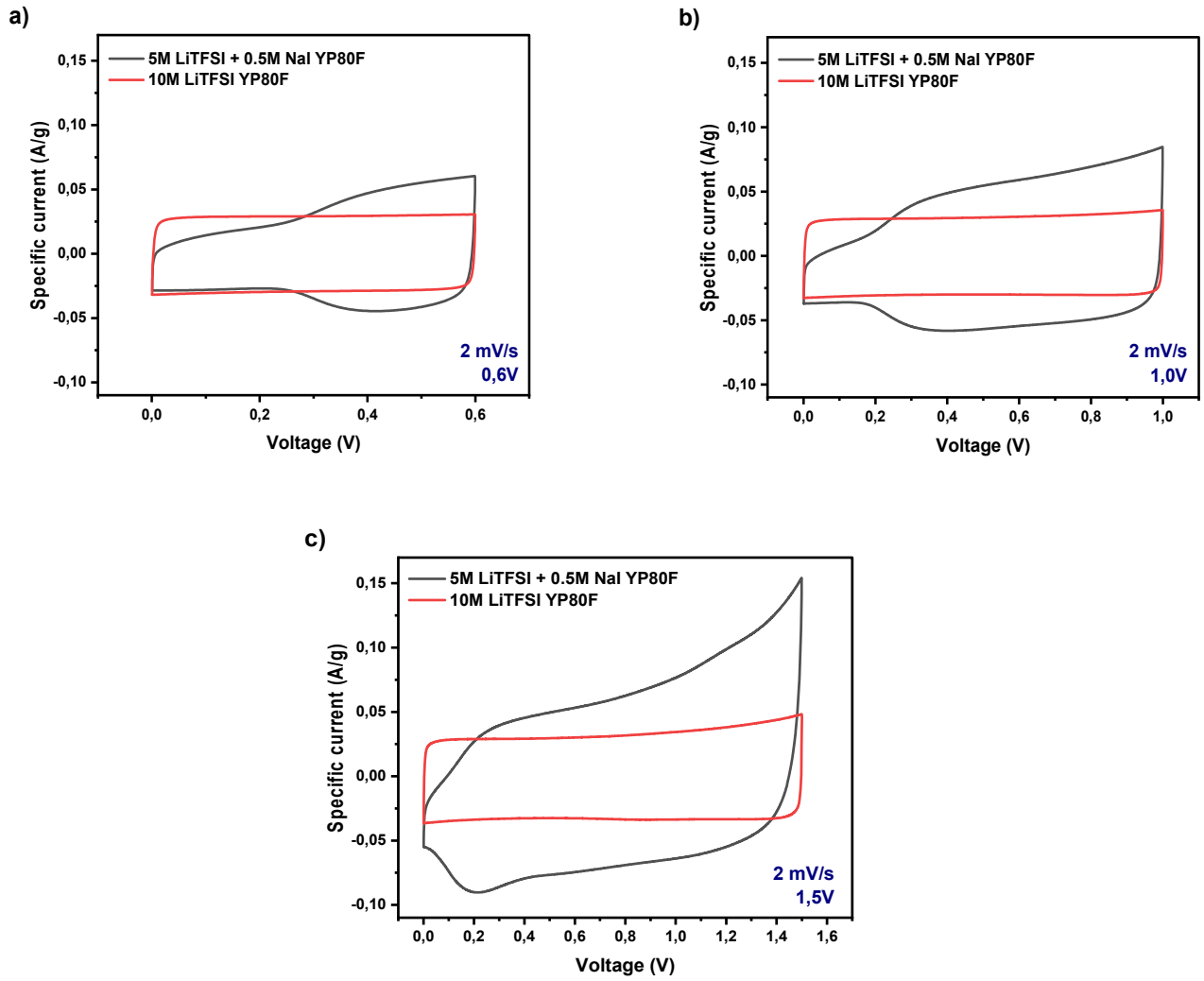

Fig. 6. Cyclic voltammetry curves of pouch cells with 5 M LiTFSI + 0.5 M NaI and 10 M LiTFSI electrolytes at a scan rate of 2 mV/s in different voltage ranges: a) 0.6 V; b) 1.0 V; c) 1.5 V.

tion of NaI significantly increases the specific capacitance and energy density due to the hybrid charge storage mechanism, while pure LiTFSI forms a system with outstanding stability and reversibility but lower capacitance.

The galvanostatic charge-discharge (GCPL) allows quantitative assessment of the capacitive characteristics, energy efficiency, and stability of supercapacitor cells. In this work, measurements were performed at a current density of 0.2 A/g in the voltage range from 0.6 to 1.5 V. The results are shown in Fig. 7. The charge-discharge curves for the 5 M LiTFSI + 0.5 M NaI electrolyte (Fig. 7a) remain almost triangular throughout the entire voltage range studied, indicating low internal resistance and high reversibility of the processes. At the same time, with an increase in the upper voltage limit, the discharge part of the curves lengthens significantly, which indicates an increase in the accumulated charge.

Quantitative data show that the specific capacitance increases from 73 F/g at 0.6 V to 128 F/g at 1.5 V. This increase is due to the active involvement of I^-/I_2 redox processes, which begin to manifest themselves at voltages above 1.0 V. Thus, the system demonstrates a transition from classic EDLC behavior to hybrid charge accumulation with a significant contribution from pseudocapacitance. Coulombic efficiency remains high across the entire voltage range (≈98%), confirming good process reversibility and minimal energy losses. It is particularly important that even at 1.5 V, efficiency does not decrease, which indicates the stability of the system in an extended voltage window.

The energy characteristics also confirm the promise of the hybrid electrolyte. The specific energy increases from 0.75 W·h/kg at 0.6 V to 9.26 W·h/kg at 1.5 V. Such a significant increase is explained not only by the quadratic dependence of energy on volt-

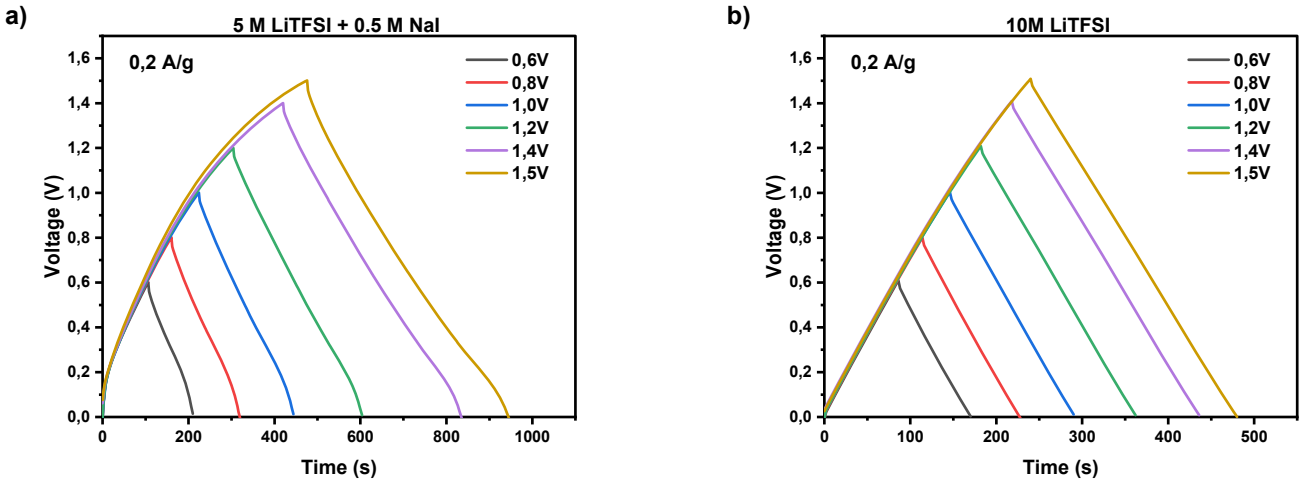

Fig. 7. Galvanostatic charge-discharge curves at a current density of 0.2 A/g for a cell with a) 5 M LiTFSI + 0.5 M NaI; b)10 M LiTFSI electrolytes in different voltage ranges.

age, but also by the additional contribution of redox reactions that enhance charge accumulation. This indicates the high potential applicability of hybrid systems in devices where a combination of energy density and stability is required. The charge-discharge curves for the 10 M LiTFSI electrolyte (Fig. 7b) also have a symmetrical and linear shape over the entire voltage range, confirming the dominance of the classical EDLC mechanism. Unlike the NaI system, there are no signs of redox processes on the curves, even at voltages above 1.0 V. The specific capacitance increases moderately: from 58 F/g at 0.6 V to 64 F/g at 1.5 V. The specific energy also increases from 0.62 W·h/kg to 4.79 W·h/kg, which is almost half the values for the hybrid electrolyte. Nevertheless, the key advantage of this system is its exceptional stability: Coulombic efficiency remains above 95% across the entire range and exceeds 98% at voltages above 0.8 V. This confirms the minimal losses and high durability of the system. Even at 1.5 V, the curves remain clearly symmetrical and stable, making the 10 M LiTFSI electrolyte the benchmark for durability, despite its relatively low specific capacitance and energy.

A comparison of the GCPL curves demonstrates (Fig. 8) a fundamental difference in the behavior of the two systems. The 5 M LiTFSI + 0.5 M NaI electrolyte provides almost twice the advantage in specific capacitance and energy due to a hybrid charge storage mechanism involving I^-/I_2 redox processes. At the same time, it maintains high efficiency and stability even at a voltage of 1.5 V.

Figure 8a shows that in the narrow voltage window of 0.6 V, the NaI containing system already exhibits longer discharge times, indicating enhanced charge storage. This trend is further confirmed at 1.0 V (Fig. 8b), where the plateau region becomes more pronounced for the hybrid electrolyte. At 1.5 V (Fig. 8c), the extended discharge profile clearly demonstrates the sustained redox contribution of the I^-/I_2, resulting in significantly prolonged discharge times compared to the purely EDL based 10 M LiTFSI system.

The electrochemical performance of the developed pouch cell supercapacitors was compared with state-of-the-art aqueous systems reported in the literature. Conventional aqueous electric double-layer capacitors typically deliver energy densities in the range of 3–8 W·h/kg, while advanced systems employing highly concentrated or redox-active electrolytes can reach values up to 10–15 W·h/kg. In this work, the pouch cell with 5 M LiTFSI + 0.5 M NaI electrolyte achieves an energy density of 9.26 W·h/kg at 1.5 V, which places it among the higher-performing aqueous supercapacitor systems. This improvement is attributed to the contribution of reversible I^-/I_2 redox reactions, which enhance charge storage beyond the electric double-layer mechanism. In contrast, the system based on 10 M LiTFSI exhibits typical electric double-layer behavior with a lower capacitance of 64 F/g but superior Coulombic efficiency (>99%) and stability. Such behavior is consistent with previously reported “water-in-salt” electrolytes, where high salt concentration suppresses water activity and improves electrochemical stability. Therefore, the proposed systems demonstrate a trade-off between energy density and long-term stability. The NaI-containing electrolyte is more suitable for high-energy applications, whereas the concentrated LiTFSI system is preferable for applications requiring excellent cycling stability and reversibility.

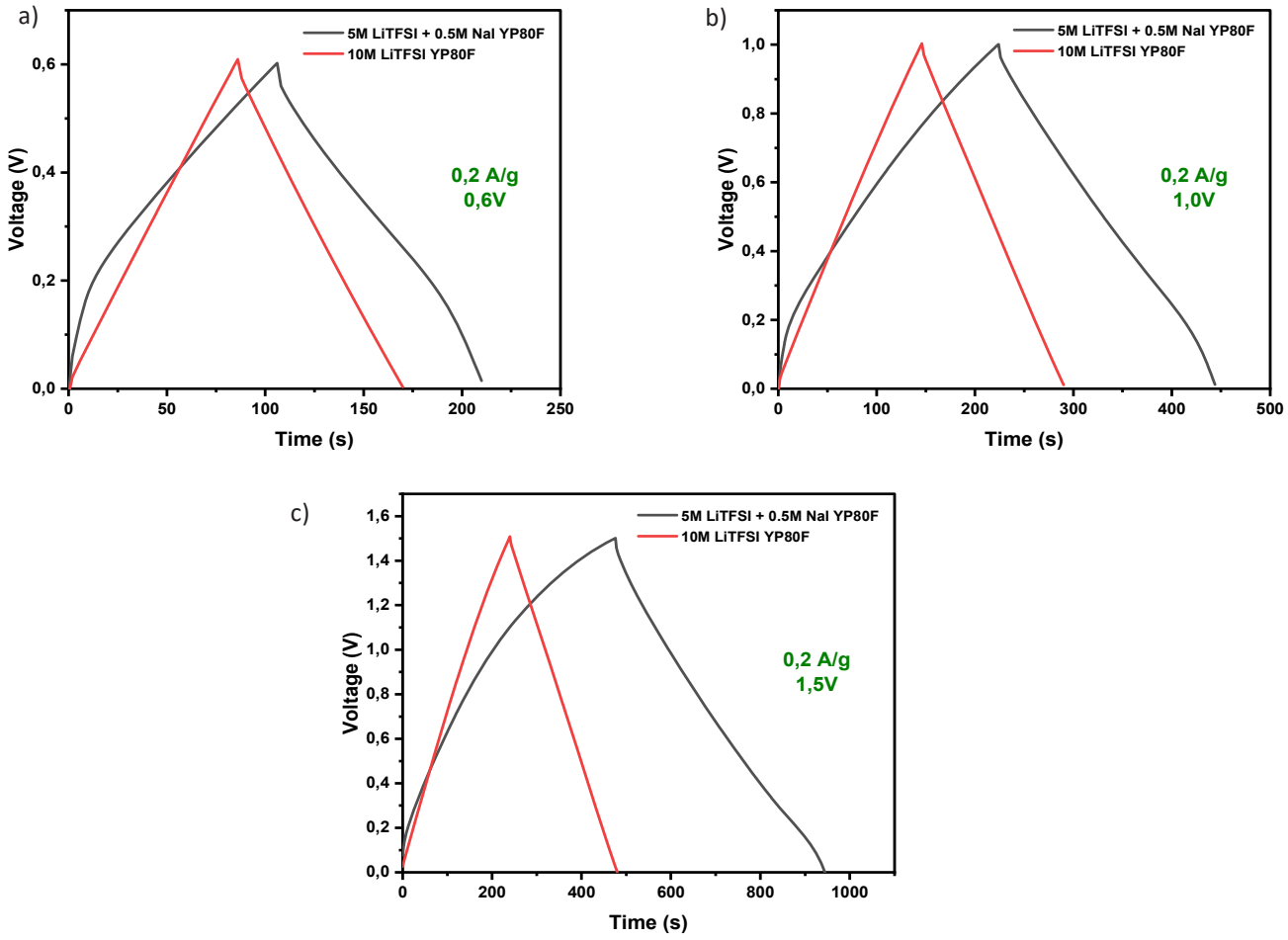

Fig. 8. Galvanostatic charge-discharge curves at a current density of 0.2 A/g for cells with 5 M LiTFSI + 0.5 M NaI and 10 M LiTFSI electrolytes in different voltage ranges.

The 10 M LiTFSI electrolyte, on the other hand, demonstrates moderate capacitance and energy values but is characterized by exemplary stability and high reversibility. It can be considered a reference EDLC system for long-term operation, while the hybrid electrolyte is preferable in cases where high energy density is critical. Self-discharge is an important parameter in evaluating the performance characteristics of supercapacitors, as it determines the device's ability to retain stored energy during storage without an external load. To evaluate the self-discharge of the systems under study, the dependence of voltage on time was measured after charging the cells to 0.6 V and 1.5 V. The results are shown in Fig. 9.

For cells with 5 M LiTFSI + 0.5 M NaI electrolyte (Fig. 9a), a faster voltage drop is observed at both 0.6 V and 1.5 V. At low voltage (0.6 V), the voltage difference over 30 h was ΔU = 0.44 V, which is higher than for cells with 10 M LiTFSI (ΔU = 0.28 V). At 1.5 V, self-discharge is even more pronounced: the voltage drop reaches ΔU = 0.95 V compared to 0.76 V for LiTFSI. The high self-discharge rate in the hybrid system is explained by the presence of I^-/I_2 redox processes, which, on the one hand, provide an increase in capacitance, but on the other hand, lead to additional discharge paths due to the chemical equilibrium of ions and possible side reactions. Thus, the addition of NaI increases the energy capacity of the system but reduces its ability to retain charge during long-term storage.

The 10 M LiTFSI-based system (Fig. 9b) demonstrates more stable voltage retention. At 0.6 V, the drop is ΔU = 0.28 V, and at 1.5 V, it is ΔU = 0.76 V, which is significantly lower than in the hybrid system. Long-term voltage retention confirms high stability and minimal involvement of side processes. This is consistent with the pure EDLC mechanism characteristic of this electrolyte. The floating test was conducted to evaluate the long-term stability of pouch-type supercapacitor cells under constant voltage conditions. In this experiment, the cells were charged to 1.5 V and held for 10 h, while the leakage current was continuously recorded. The results are shown in Fig. 10.

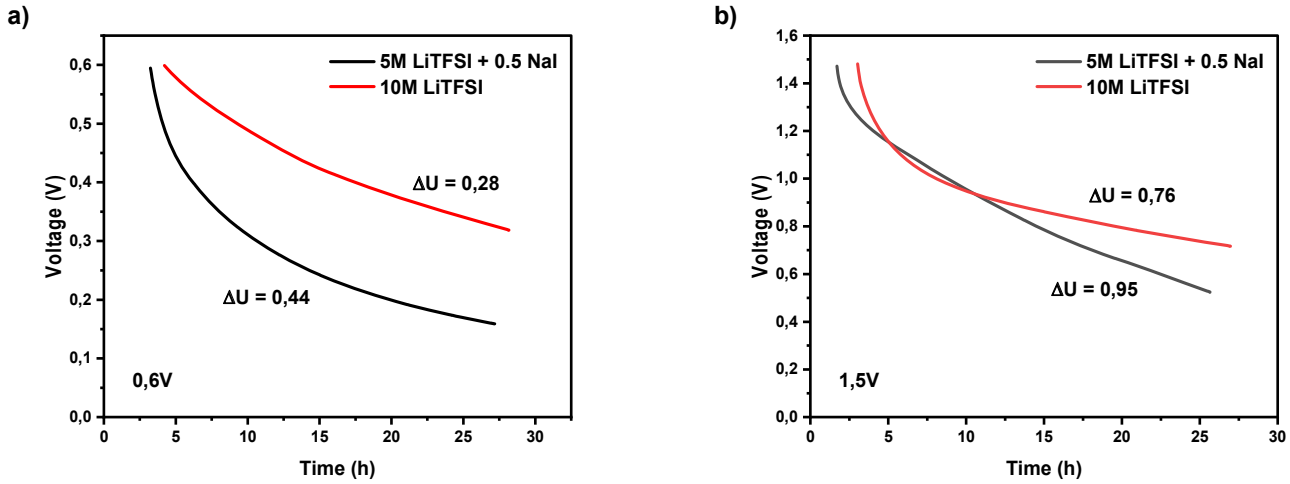

Fig. 9. Voltage dependence on time (self-discharge) for cells with 5 M LiTFSI + 0.5 M NaI and 10 M LiTFSI electrolytes over 24 h: a) charging to 0.6 V; b) charging to 1.5 V.

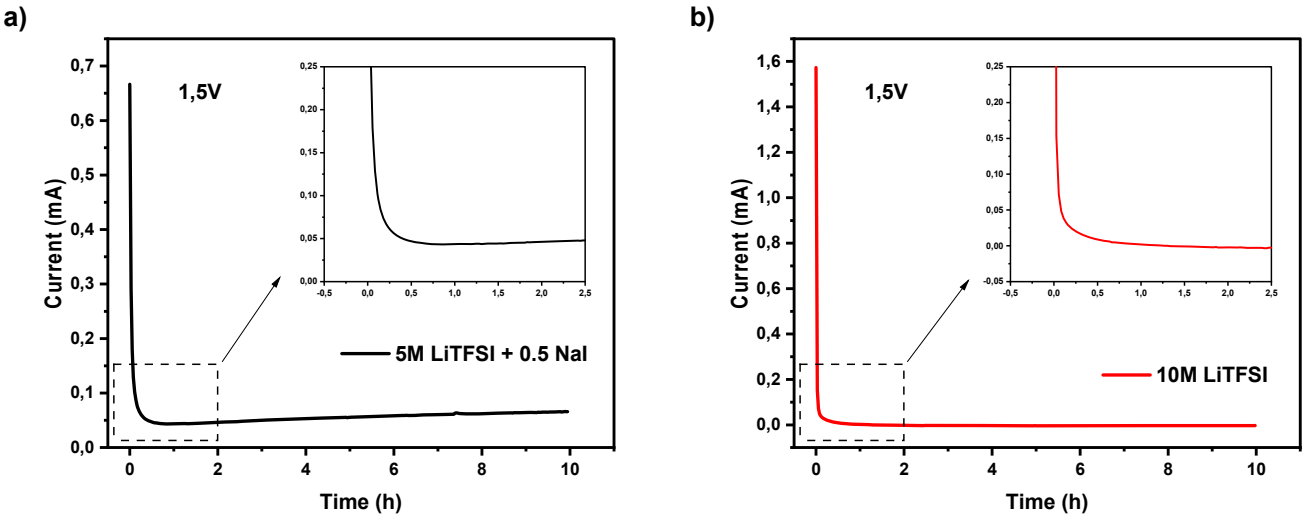

Fig. 10. Floating test of pouch cells at 1.5 V for 10 h: a) 5 M LiTFSI + 0.5 M NaI; b) 10 M LiTFSI electrolytes.

When held at a voltage of 1.5 V, the hybrid system with 5 M LiTFSI + 0.5 M NaI (Fig. 10a) demonstrated a moderate initial leakage current of approximately 0.7 mA, which rapidly decreased within the first hour of testing and stabilized around 0.04 mA. This rapid decay indicates the formation of a quasi-equilibrium state between the electrode surface and the electrolyte. However, a slight increase in current was observed at longer retention times, which may be associated with slow redox transitions of the I^-/I_2 couple and diffusion-limited ion rearrangements. These processes are characteristic of hybrid systems where the pseudocapacitive contribution enhances the overall energy storage but may slightly affect long-term stability at elevated potentials.

In contrast, the system with 10 M LiTFSI (Fig. 10b) exhibited a higher initial current peak of approximately 1.5 mA, followed by a rapid decay to a low and stable current of about 0.01 mA. This behavior suggests that, although the concentrated LiTFSI electrolyte initially experiences a stronger current surge, it quickly stabilizes due to the absence of redox-active species and the dominance of purely capacitive charge storage mechanisms. The absence of a secondary current rise during the 10 h retention period confirms the excellent electrochemical stability of this electrolyte under prolonged polarization conditions.

4. Conclusion

A comparative analysis of the electrochemical characteristics of supercapacitor pouch cells based on YP 80F carbon material was carried out using two types of aqueous electrolytes: 5 M LiTFSI + 0.5 M NaI and 10 M LiTFSI. It was shown that the addition of NaI to the electrolyte forms a hybrid system involving I^-/I_2 redox processes, which leads to a significant increase in specific capacitance (up to 128 F/g) and specific energy (up to 9.26 W·h/kg) at a voltage of 1.5 V while maintaining high coulombic efficiency (>97%). At the same time, the use of 10 M LiTFSI provides typical EDL charging behavior with lower capacitance values (64.32 F/g) but high stability, process reversibility, and Coulombic efficiency >99%.

Thus, the electrolyte based on 5 M LiTFSI + 0.5 M NaI is a promising solution for applications requiring high energy density and an extended operating voltage window, while 10 M LiTFSI is preferable for tasks where durability, stability, and high efficiency are key parameters. The results confirm the effectiveness of using redox-active additives to increase the energy density of aqueous supercapacitors and open up new opportunities for their optimization depending on the target operating conditions. Further efforts are directed towards achieving higher stability and efficiency for the hybrid supercapacitor pouch cells.

Acknowledgment

This research has been funded by the Committee of Science of the Ministry of Science and Higher Education of the Republic of Kazakhstan (Grant No. BR27198045).

Authors acknowledge input from Prof. Qamar Abbas (Poznan University of Technology, Poland) related with iodide/iodine redox system in porous carbon electrodes.

References

[1]. D. Dong, Y. Xiao, Recent progress and challenges in coal-derived porous carbon for supercapacitor applications, *Chem. Eng. J.* 470 (2023) 144441. DOI: 10.1016/j.cej.2023.144441

[2]. Y. Cheng, Z. Lia, Y. Li, S. Dai, G. Ji, et al., Rationally regulating complex dielectric parameters of mesoporous carbon hollow spheres to carry out efficient microwave absorption, *Carbon* 127 (2018) 643–652. DOI: 10.1016/j.carbon.2017.11.055

[3]. X.-J. Zhang, J.-Q. Zhu, P.-G. Yin, A.-P. Guo, A.-P. Huang, et al., Tunable high-performance microwave absorption of Co_1–xS hollow spheres constructed by nanosheets within ultralow filler loading, *Adv. Funct. Mater.* 28 (2018) 1800761. DOI: 10.1002/adfm.201800761

[4]. J. Cui, Y. Xi, S. Chen, D. Li, X. She, et al., Proliferagreen-tide as sustainable source for carbonaceous aerogels with hierarchical pore to achieve multiple energy storage, *Adv. Funct. Mater.* 26 (2016) 8487–8495. DOI: 10.1002/adfm.201603933

[5]. Z.-E. Tang, S. Lim, Y.-L. Pang, H.-C. Ong, K.-T. Lee, Synthesis of biomass as heterogeneous catalyst for application in biodiesel production: State of the art and fundamental review, *Renew. Sustain. Energy Rev.* 92 (2018) 235–253. DOI: 10.1016/j.rser.2018.04.056

[6]. G. Xu, J. Han, B. Ding, P. Nie, J. Pan, et al., Biomass-derived porous carbon materials with sulfur and nitrogen dual-doping for energy storage, *Green Chem.* 17 (2015) 1668–1674. DOI: 10.1039/C4GC02185A

[7]. Z. Gao, Y. Zhang, N. Song, X. Li, Biomass-derived renewable carbon materials for electrochemical energy storage, *Mater. Res. Lett.* 5 (2017) 69–88. DOI: 10.1080/21663831.2016.1250834

[8]. H. Xu, X. Yin, M. Zhu, M. Han, Z. Hou, et al., Carbon hollow microspheres with a designable mesoporous shell for high-performance electromagnetic wave absorption, *ACS Appl. Mater. Interfaces* 9 (2017) 6332–6341. DOI: 10.1021/acsami.6b15826

[9]. Y. Ding, Z. Zhang, B. Luo, Q. Liao, S. Liu, et al., Investigation on the broadband electromagnetic wave absorption properties and mechanism of Co_3O_4-nanosheets/reduced-graphene-oxide composite, *Nano Research* 10 (2017) 980–990. DOI: 10.1007/s12274-016-1357-6

[10]. C. Luo, T. Jiao, J. Gu, Y. Tang, J. Kong, Graphene shield by SiBCN ceramic: a promising high-temperature electromagnetic wave-absorbing material with oxidation resistance, *ACS Appl. Mater. Interfaces* 10 (2018) 39307–39318. DOI: 10.1021/acsami.8b15365

[11]. B.E. Conway, Electrochemical Supercapacitors: Scientific Fundamentals and Technological Applications, Springer, 1999, 698 p.

[12]. P. Simon, Y. Gogotsi, Materials for electrochemical capacitors, *Nat. Mater*. 7 (2008) 845–854. DOI: 10.1038/nmat2297

[13]. A. Nazir, H. Yu, L. Wang, M. Haroon, R.S. Ullah, et al., Recent progress in the modification of carbon materials and their application in composites for electromagnetic interference shielding, *J. Mater.*

Sci. 53 (2018) 8699–8719. DOI: 10.1007/s10853-018-2122-x

[14]. C. Luo, Y. Tang, T. Jiao, J. Kong, High-temperature stable and metal-free electromagnetic wave-absorbing SiBCN ceramics derived from carbon-rich hyperbranched polyborosilazanes, *ACS Appl. Mater. Interfaces* 10 (2018) 28051–28061. DOI: 10.1021/acsami.8b07879

[15]. G.A. Safitri, K. Nueangnoraj, P. Sreearunothai, J. Manyam, Fabrication of activated carbon pouch cell supercapacitor: Effects of calendering and selection of separator–solvent combination, *Current Applied Science and Technology* 20 (2020) 124–135. https://li01.tci-thaijo.org/index.php/cast/article/view/234784

[16]. B.K. Chakrabarti, K.B. Dönmez, Z. Çobandede, C.T.J. Low, Practical pouch cell supercapacitor electrodes by electrophoretic deposition of activated carbon on nickel foam, *ChemElectroChem* 11 (2024) e202400244. DOI: 10.1002/celc.202400244

[17]. C. Prehal, H. Fitzek, G. Kothleitner, V. Presser, B. Gollas, et al., Persistent and reversible solid iodine electrodeposition in nanoporous carbons, *Nat. Commun*. 11 (2020) 4838. DOI: 10.1038/s41467-020-18610-6

[18]. Q. Abbas, H. Fitzek, V. Pavlenko, B. Gollas, Towards an optimized hybrid electrochemical capacitor in iodide-based aqueous redox-electrolyte: Shift of equilibrium potential by electrodes mass-balancing, *Electrochim. Acta* 337 (2020) 135785. DOI: 10.1016/j.electacta.2020.135785

[19]. Q. Abbas, H. Fitzek, H. Schröttner, S. Dsoke, B. Gollas, Immobilization of polyiodide redox species in porous carbon for battery-like electrodes in eco-friendly hybrid electrochemical capacitors, *Nanomaterials* 9 (2019) 1413. DOI: 10.3390/nano9101413

[20]. H. Fitzek, M. Sterrer, D. Knez, H. Schranger, A. Sarapulova, et al., Impact of iodine electrodeposition on nanoporous carbon electrode determined by EQCM, XPS and in situ Raman spectroscopy, *Nanomaterials* 13 (2023) 1545. DOI: 10.3390/nano13091545

[21]. Z. Mansurov, Z. Supiyeva, K. Avchukir, A. Taurbekov, M. Yeleuov, et al., Investigation of gold electrosorption onto gold and carbon electrodes using an electrochemical quartz crystal microbalance, *Eurasian Chem.-Technol. J.* 21 (2019) 283–289. DOI: 10.18321/ectj885

[22]. Z. Supiyeva, Z. Mansurov, S. Azat, Q. Abbas, A unique choline nitrate-based organo-aqueous electrolyte enables carbon/carbon supercapacitor operation in a wide temperature window (−40 °C to 60 °C), *Front. Chem*. 12 (2024). DOI: 10.3389/fchem.2024.1377144

[23]. V. Pavlenko, Z. Supiyeva, Application of carbons produced from rice husk in the process of capacitive deionization, *Eurasian Chem.-Technol. J.* 22 (2020) 277–284. DOI: 10.18321/ectj996

[24]. K. Askaruly, Z. Supiyeva, S. Azat, Y. Yeszhan, X. Pan, et al., From electrochemical performance to mechanical issues: A review on silicon anode architectures for advanced lithium-ion batteries, *J. Power Sources* 659 (2025) 238423. DOI: 10.1016/j.jpowsour.2025.238423